Available online at www.sciencedirect.com
SCIENCE DIRECT
Journal of Solid State Chemistry 179 (2006) 1883–1891
JOURNAL OF SOLID STATE CHEMISTRY
www.elsevier.com/locate/jssc

Rapid Communication

Synthesis, crystal structure and spectroscopy properties of $Na_3AZr(PO_4)_3$ (A = Mg, Ni) and $Li_{2.6}Na_{0.4}NiZr(PO_4)_3$ phosphates

M. Chakir[a,*], A. El Jazouli[a], D. de Waal[b]

[a]LCMS, UFR Sciences des Matériaux Solides, Faculté des Sciences Ben M'Sik, UH2M, Avenue Idriss El Harti, BP 7955, Casablanca, Morocco
[b]Department of Chemistry, University of Pretoria, 0002 Pretoria, South Africa

Received 18 October 2005; received in revised form 6 March 2006; accepted 8 March 2006
Available online 19 April 2006

Abstract

$Na_3AZr(PO_4)_3$ (A = Mg, Ni) phosphates were prepared at 750 °C by coprecipitation route. Their crystal structures have been refined at room temperature from X-ray powder diffraction data using Rietveld method. $Li_{2.6}Na_{0.4}NiZr(PO_4)_3$ was synthesized through ion exchange from the sodium analog. These materials belong to the Nasicon-type structure. Raman spectra of $Na_3AZr(PO_4)_3$ (A = Mg, Ni) phosphates present broad peaks in favor of the statistical distribution in the sites around PO_4 tetrahedra. Diffuse reflectance spectra indicate the presence of octahedrally coordinated Ni^{2+} ions.

Keywords: Structure; Nasicon; X-ray diffaction; Raman

1. Introduction

Nasicon-type materials with general formula $M_nA_2(PO_4)_3$ have been extensively studied in the context of various fields of solid state chemistry: solid electrolytes [1], electrode materials [2], low thermal expansion ceramics [3], etc. Their structure [4] consists of a three-dimensional network built up of PO_4 tetrahedra sharing corners with AO_6 octahedra. In this skeleton, there are two sites, usually labeled $M(1)$ and $M(2)$. The $M(1)$ site is an antiprism formed by the triangular faces of two AO_6 octahedra along c-axis of the hexagonal cell. Thus the network of the $NaA_2(PO_4)_3$ can be considered as made up of infinite ribbons of composition $(O_3AO_3M1O_3AO_3)_\infty$ connected by PO_4 tetrahedra. The $M(2)$ sites are located between these ribbons in large cavities with a eight-fold coordination. The $M(1)$ and $M(2)$ sites may be completely empty as in $NbZr(PO_4)_3$ [5], partially occupied as in $NaZr_2(PO_4)_3$ [4], $Na_3CaTi(PO_4)_3$ [6], and $Na_3MgTi(PO_4)_3$ [7], or full as in $Na_5Ti(PO_4)_3$ [8], $Na_5Zr(PO_4)_3$ [9], and $Na_{4.5}Yb_{1.5}(PO_4)_3$ [10]. Recently, a neutron diffraction investigation by Masquelier's group shows that in the two rhombohedral Nasicon $Li_3Fe_2(PO_4)_3$ and $Li_3V_2(PO_4)_3$, lithium ions are distributed on a new four-fold-coordinated site that they label $M(3)$ [11,12]. In this site, the lithium atoms surround only the $M(1)$ ($3a$) site and are arranged in a tetrahedral environment.

The compound $Na_3MgZr(PO_4)_3$ has been already prepared [13], but its structure has not been determined. Crystal data and ionic conductivity have been reported for the $Na_{1+x}Mg_{x/2}Zr_{2-x/2}(PO_4)_3$ ($0 \leqslant x \leqslant 2$) compositions prepared by solid-state reaction [14]. We showed recently by coprecipitation method that the solid solutions $Na_{1+x}A_{x/2}Zr_{2-x/2}(PO_4)_3$ (A = Mg, Ni) exist in the range of ($0 \leqslant x \leqslant 3$) [15].

The present paper reports on the preparation of $Na_3MgZr(PO_4)_3$ and $Na_3NiZr(PO_4)_3$ by coprecipitation method, the refinement of their crystal structure from X-ray powder diffraction patterns and on their characterization by Raman and UV-visible spectroscopies. Synthesis and X-ray diffraction (XRD) results of a new $Li_{2.6}Na_{0.4}NiZr(PO_4)_3$ phosphate are also reported.

2. Experimental

$Na_3AZr(PO_4)_3$ (A = Mg, Ni) phosphates were obtained by coprecipitation route from Na_2CO_3(I) dissolved in

*Corresponding author. Fax: +212 22 70 46 75.
E-mail address: fachakir@yahoo.fr (M. Chakir).

0022-4596/$ - see front matter © 2006 Elsevier Inc. All rights reserved.
doi:10.1016/j.jssc.2006.03.003

dilute nitric acid solution and aqueous solutions of ($ZrOCl_2 \cdot 8H_2O$)(II), ($A(NO_3)_2 \cdot 6H_2O$)(III) (A = Mg, Ni) and ($NH_4)_2HPO_4$(IV) as starting materials (all solutions were prepared in stoichiometric proportions). A slow addition of (IV) in (I + II + III) mixture at room temperature induces the formation of a gel. After drying at 60 °C, the resulting powder was progressively heated in air at 200 °C (24 h), 400 °C (24 h), 600 °C (24 h) and 750 °C (24 h) with intermitting regrinding. The powder of $Na_3MgZr(PO_4)_3$ is white while that of $Na_3NiZr(PO_4)_3$ is yellow.

$Li_{2.6}Na_{0.4}NiZr(PO_4)_3$ can be obtained from $Na_3NiZr(PO_4)_3$ after ion exchange in molten $LiNO_3$. To favor ion exchange, the weight ratio $LiNO_3/Na_3NiZr(PO_4)_3$ was set to >10, and the mixture was maintained for 3 h at 300 °C. The final ion-exchange solid was washed repeatedly with distilled water to eliminate the (Li, Na)NO_3 compounds before drying overnight at 60 °C. Chemical analysis revealed that the $Na^+ \leftrightarrow Li^+$ ion-exchange was not complete: the final product presented the formula $Li_{2.6}Na_{0.4}NiZr(PO_4)_3$. Its purity and lattice parameters determination were carefully monitored by XRD on a Panalytical X'Pert PRO diffractometer (Co$K\alpha$ radiation). Diffraction data of $Na_3AZr(PO_4)_3$ (A = Mg, Ni) phosphates were collected at room temperature on a Siemens D 5000 diffractometer.

Raman spectra were recorded using a Dilor XY Raman microprobe. The samples were excited with the 514.5 nm line of an argon ion laser (Coherent model Innova 300). The spectral resolution was 3 cm^{-1}, the laser output power 110 mW, and the integration time 30 s. Absorption spectra were recorded using a double monochromator Cary 2400 spectrometer at 300 K.

3. Results and discussion

3.1. Rietveld refinement and structure study of $Na_3AZr(PO_4)_3$ (A = Mg, Ni)

The X-ray powder diffraction data show that $Na_3AZr(PO_4)_3$ (A = Mg, Ni) phosphates crystallize in the trigonal system (S. G. $R\bar{3}c$). Assuming that $Na_3MgZr(PO_4)_3$ and $Na_3NiZr(PO_4)_3$ belong to the Nasicon family, the Zr(A), P and O atoms are in the (12c), (18e) and (36f) Wyckoff positions, respectively, of the $R\bar{3}c$ space group. The initial atomic coordinates used for the refinement of the crystal structure of $Na_3MgZr(PO_4)_3$ were those of $Na_{4.5}Yb_{1.5}(PO_4)_3$ [10]. $Na_3MgZr(PO_4)_3$ was then used as a model to refine the structure of $Na_3NiZr(PO_4)_3$. Na atoms were assumed to occupy the M(1) and M(2) sites. In the first step, Na occupy fully the M(1) site and the excess of sodium (two atoms) was located in the M(2) site (18e). These refinements lead to a rather good agreement between the experimental and calculated XRD patterns and to follow reliability factors [R_p = 11%, R_{wp} = 14% and R_B = 6% for $Na_3MgZr(PO_4)_3$, and R_p = 8%, R_{wp} = 11% and R_B = 5% for $Na_3NiZr(PO_4)_3$]. In the second step, the occupancies of Na(1) and Na(2) sites were allowed to vary, but the total sodium contents were constrained to 3. The result of these refinements show clearly a partial occupancy of M(1) and M(2) sites. The crystallographic formulas are $[Na_{2.11}\square_{0.89}]_{M2}[Na_{0.89}\square_{0.11}]_{M1}[MgZr]_A(PO_4)_3$ and $[Na_{2.09}\square_{0.91}]_{M2}[Na_{0.91}\square_{0.09}]_{M1}[NiZr]_A(PO_4)_3$. The same distribution was already shown for $Na_2SnFe(PO_4)_3$ phosphate [16]. On the other hand, and in order to confirm the cationic distributions already obtained, the structural refinement of $Na_3AZr(PO_4)_3$ (A = Mg, Ni) was undertaken assuming that Na atoms were distributed also in M(3) sites. This refinement leads to high displacement parameters and/or to unacceptable P–O distances values.

The experimental conditions and the results of the refinements as well as different structural parameters are given in Tables 1 and 2. Figs. 1 and 2 show observed, calculated and different X-ray profiles for $Na_3MgZr(PO_4)_3$ and $Na_3NiZr(PO_4)_3$.

The structure of $Na_3AZr(PO_4)_3$ (A = Mg, Ni) is based on a three-dimensional framework of PO_4 tetrahedra and $(Zr/A)O_6$ octahedra sharing corners (Fig. 3). Zr^{4+} and A^{2+} ions occupy statistically the 12c sites. Na^+ cations occupy partially the M(1) and M(2) sites. Zr/A (A = Mg, Ni) atoms are displaced from the center of the octahedron due to the Na^+–Zr^{4+}/A^{2+} repulsions. Consequently the Zr/A–O(2) distance (2.097 Å for Zr/Mg and 2.100 Å for

Table 1
Conditions and results of the Rietveld refinement of $Na_3AZr(PO_4)_3$ (A = Mg, Ni)

Composition	$Na_3MgZr(PO_4)_3$	$Na_3NiZr(PO_4)_3$
Wavelength (Å)	$\lambda k\alpha_1$ = 1.5406; $\lambda k\alpha_2$ = 1.5444	
Step width (°2θ); angular range (°)	0.04; 10–100	0.02; 10–100
Zero point (°2θ)	0.162(1)	−0.065(2)
Pseudo-Voigt function	η = 0.522(4)	η = 0.469(2)
Half-width parameters: U, V, W	0.238(1), −0.099(1), 0.051(1)	0.196(3), −0.067(2), 0.033(2)
Number of reflections	398	363
System; space group; Z	Trigonal; $R\bar{3}c$; 6	
a (Å); c (Å)	8.9095(4); 22.255(1)	8.8909(4); 22.225(1)
V (Å^3)	1529.9(1)	1521.5(1)
R_B; R_p; R_{wp}	0.06; 0.12; 0.13	0.05; 0.11; 0.13

Table 2
Atomic coordinates and isotropic temperature factors in $Na_3AZr(PO_4)_3$ (A = Mg, Ni)

Atom	Wyckoff site	x	y	z	B_{iso} (Å^2)	Occ.
$Na_3MgZr(PO_4)_3$						
Zr/Mg	12*c*	0	0	0.1474(1)	0.5(1)	1
Na(1)	6*b*	0	0	0	4.8(6)	0.89(2)
Na(2)	18*e*	0.6400(9)	0	0.2500	5.4(8)	0.703(1)
P	18*e*	0.2935(4)	0	0.2500	1.1(3)	1
O(1)	36*f*	0.1852(6)	−0.0250(6)	0.1942(2)	0.8(4)	1
O(2)	36*f*	0.1926(5)	0.1725(6)	0.0883(3)	1.0(5)	1
$Na_3NiZr(PO_4)_3$						
Zr/Ni	12*c*	0	0	0.1474(1)	0.9(2)	1
Na(1)	6*b*	0	0	0	4.2(7)	0.91(1)
Na(2)	18*e*	0.6340(14)	0	0.2500	6.3(3)	0.697(1)
P	18*e*	0.2934(5)	0	0.2500	0.9(3)	1
O(1)	36*f*	0.1865(9)	−0.0249(10)	0.1941(3)	1.1(4)	1
O(2)	36*f*	0.1908(7)	0.1717(8)	0.0872(3)	1.1(4)	1

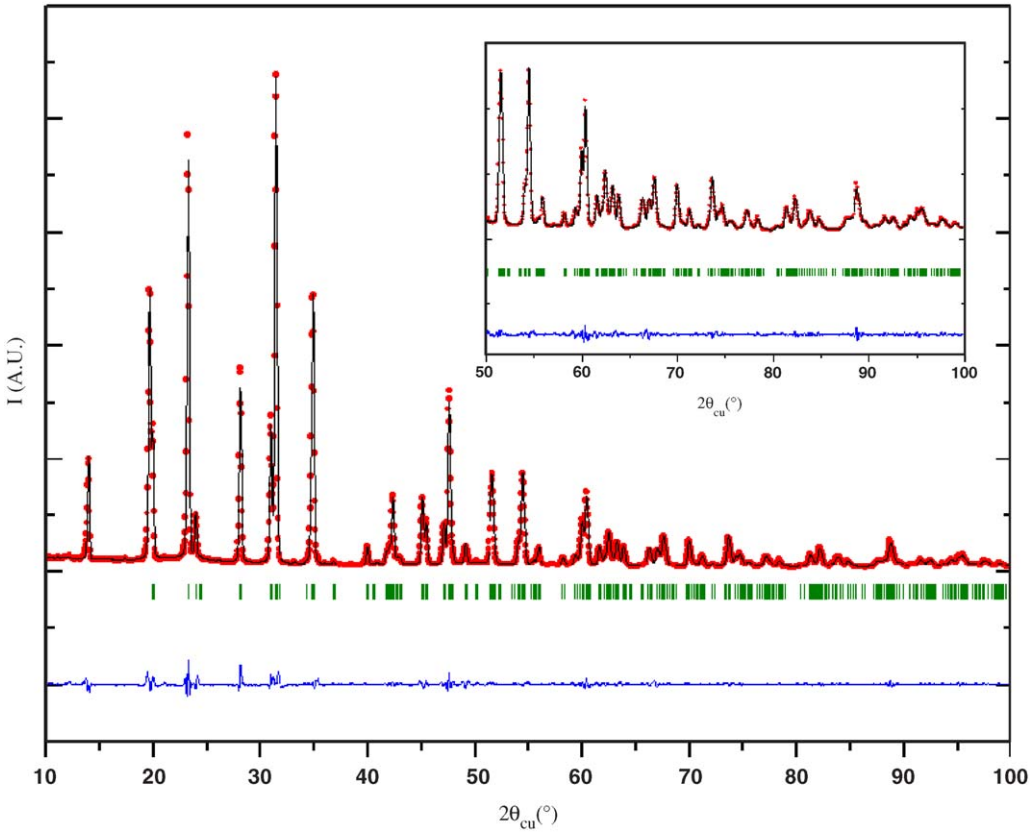

Fig. 1. Observed (…), calculated (—) and different powder diffraction patterns of $Na_3MgZr(PO_4)_3$.

Zr/Ni), neighboring the sodium Na(1), is slightly greater than the Zr/A–O(1) distance (2.055 Å for Zr/Mg and 2.059 Å for Zr/Ni) (Tables 3 and 4). The average Zr/A–O distances (2.076 Å for Zr/Mg and 2.080 Å for Zr/Ni) are slightly smaller than the values calculated from the ionic radii (2.12 Å for Zr/Mg and 2.11 Å for Zr/Ni) [17]. The O–(Zr/A)–O angles vary between 84.8° and 171.5° for Zr/Mg and between 83.7° and 170.6° for Zr/Ni. The angles implying the shortest bonds are superior to those involving the longest ones as a consequence of the O–O repulsions which are stronger for O(1)–O(1) than for O(1)–O(2) and O(2)–O(2). Zr/A–Zr/A distance along c-axis (4.566 Å for Mg and 4.559 Å for Ni) is inferior to the Zr–Zr distance in $NaZr_2(PO_4)_3$ (4.752 Å) due to the cationic repulsions between ions in 12c sites. These repulsions are stronger in $NaZr_2(PO_4)_3$ (charge of $Zr^{4+} = 4$) than in $Na_3AZr(PO_4)_3$ (mean charge of $Zr^{4+}/A^{2+} = 3$).

The P–O distances values [(1.519; 1.532 Å) for $Na_3MgZr(PO_4)_3$ and (1.512; 1.540 Å) for $Na_3NiZr(PO_4)_3$] are close to those typically found in Nasicon-like

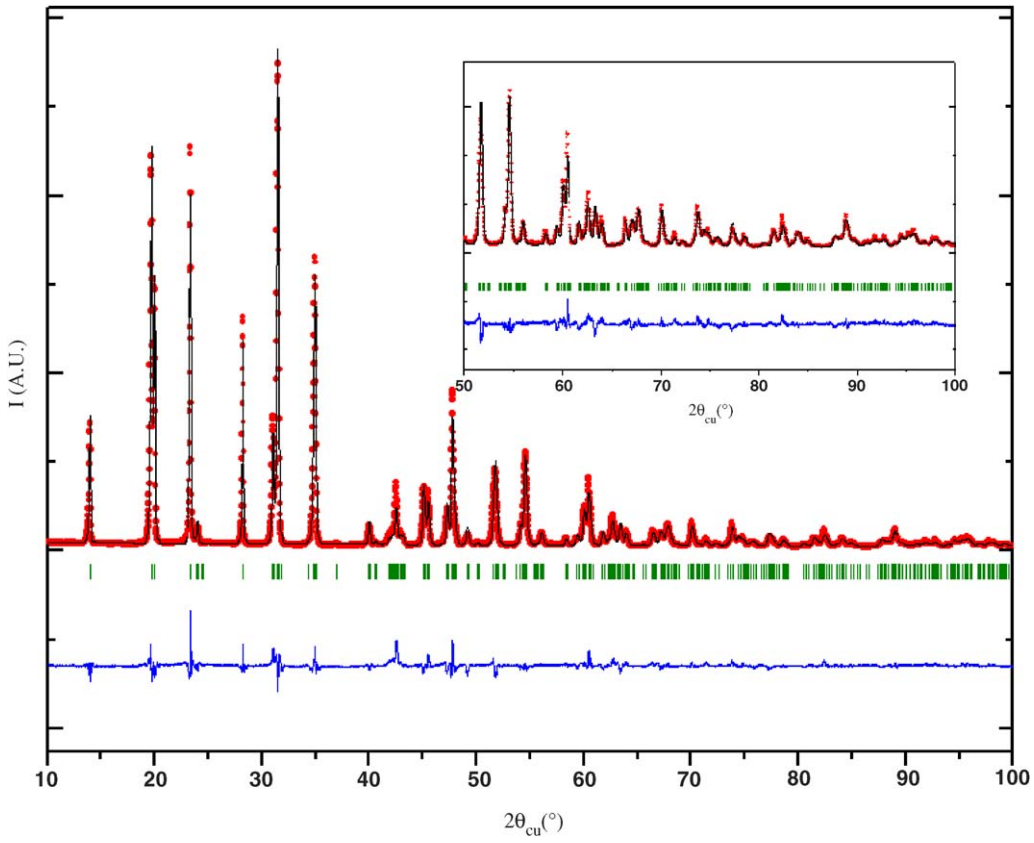

Fig. 2. Observed (…), calculated (—) and different powder diffraction patterns of $Na_3NiZr(PO_4)_3$.

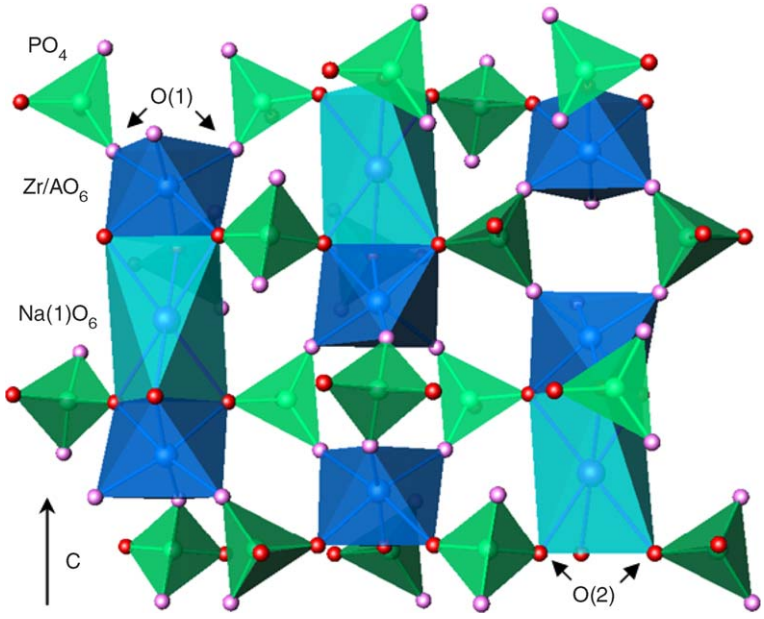

Fig. 3. Structure of $Na_3AZr(PO_4)_3$ (A = Mg, Ni) phosphates.

phosphates. O–P–O angles vary from 106.4° to 111.7° for $Na_3MgZr(PO_4)_3$ and from 105.6° to 112.5° for $Na_3NiZr(PO_4)_3$. The Na(1) atoms occupy the center of the $M(1)$ site. Na(1)–O(2) distance (Tables 3 and 4) (2.555 Å for $Na_3MgZr(PO_4)_3$ and 2.525 Å for $Na_3NiZr(PO_4)_3$) is larger than the calculated one (2.42 Å) from the ionic radii [17]. The Na(2) atoms, located in the $M(2)$ site, are surrounded by eight oxygen atoms, the Na(2)–O distances vary from 2.449 to 2.872 Å for $Na_3MgZr(PO_4)_3$ and from 2.457 to 2.909 Å for $Na_3NiZr(PO_4)_3$. The ionic character of the

Table 3
Bond distances and angles for $Na_3MgZr(PO_4)_3$

Bond distances (Å)		Angles (deg)	
(Zr/Mg)–O(1) × 3	2.055(5)	O(1)–(Zr/Mg)–O(1)	96.6(3)
(Zr/Mg)–O(2) × 3	2.097(5)	O(1)–(Zr/Mg)–O(2)	88.4(3); 89.4(3); 171.5(4)
P–O(1) × 2	1.519(5)	O(2)–(Zr/Mg)–O(2)	84.8(3)
P–O(2) × 2	1.532(5)	O(1)–P–O(1)	111.6(4)
Na(1)–O(2) × 6	2.555(4)	O(1)–P–O(2)	106.4(5); 111.7(5)
Na(2)–O(1) × 2	2.872(8)	O(2)–P–O(2)	108.7(4)
Na(2)–O(1) × 2	2.697(5)	O(2)–Na(1)–O(2)	67.2(2); 112.7(3); 180.0(4)
Na(2)–O(2) × 2	2.524(8)	O(1)–Na(2)–O(1)	82.4(2); 85.8(3); 111.6(3); 157.2(3)
Na(2)–O(2) × 2	2.449(4)	O(1)–Na(2)–O(2)	53.9(2); 67.3(2); 114.8(3); 151.6(4)
		O(2)–Na(2)–O(2)	59.1(3); 69.3(3); 128.4(4); 162.1(3)

Table 4
Bond distances and angles for $Na_3NiZr(PO_4)_3$

Bond distances (Å)		Angles (deg)	
(Zr/Ni)–O(1) × 3	2.059(8)	O(1)–(Zr/Ni)–O(1)	96.8(6)
(Zr/Ni)–O(2) × 3	2.100(7)	O(1)–(Zr/Ni)–O(2)	88.8(1); 89.9(1); 170.6(3)
P–O(1) × 2	1.512(8)	O(2)–(Zr/Ni)–O(2)	83.7(2)
P–O(2) × 2	1.540(7)	O(1)–P–O(1)	112.4(2)
Na(1)–O(2) × 6	2.525(7)	O(1)–P–O(2)	105.6(2); 112.5(2)
Na(2)–O(1) × 2	2.909(7)	O(2)–P–O(2)	108.1(8)
Na(2)–O(1) × 2	2.677(12)	O(2)–Na(1)–O(2)	67.4(5); 112.5(5); 180.0
Na(2)–O(2) × 2	2.457(7)	O(1)–Na(2)–O(1)	81.4(6); 85.1(1); 110.6(7); 159.6(6)
Na(2)–O(2) × 2	2.463(13)	O(1)–Na(2)–O(2)	53.2(4); 69.7(4); 114.6(6); 152.4(7)
		O(2)–Na(2)–O(2)	60.8(3); 69.4(5); 130.2(5); 160.3(1)

Na–O bonds explains the high conductivity found for $Na_3MgZr(PO_4)_3$ [14], and the values of isotropic temperature factors obtained for Na atoms in $M(1)$ and $M(2)$ sites.

Calculated valences ($S_i = \Sigma\exp[(R_{ij}-d_{ij})/b]$ with $b = 0.37$ Å) based on bond strength analysis [18] [P: 5.14, Zr: 4.01, Mg: 2.12, Na(1): 0.80, Na(2): 0.92 for $Na_3MgZr(PO_4)_3$ and P: 4.94, Zr: 4.11, Ni: 1.91, Na(1): 0.86, Na(2): 0.94 for $Na_3NiZr(PO_4)_3$] are in good agreement with the expected formal oxidation states of P^{5+}, Zr^{4+}, Mg^{2+}, Ni^{2+} and Na^+.

3.2. Crystallochemical study

The X-ray powder patterns of $Na_3AZr(PO_4)_3$ (A = Mg, Ni) can be indexed assuming a hexagonal cell parameters: $a_h = 8.9095(4)$ Å; $c_h = 22.255(1)$ Å for $Na_3MgZr(PO_4)_3$ and $a_h = 8.8909(4)$ Å; $c_h = 22.225(1)$ Å for $Na_3NiZr(PO_4)_3$. All of the observed reflections are compatible with the $R\bar{3}c$ space group. Contrary to the pure sodium composition, $Li_{2.6}Na_{0.4}NiZr(PO_4)_3$ X-ray pattern was indexed in $R\bar{3}c$ space group. Indeed, XRD pattern (Fig. 4) clearly shows reflections such as (102) ($2\theta_{CoK\alpha} \approx 16.5°$) and (303) ($2\theta_{CoK\alpha} \approx 44.9°$) which are normally forbidden in the $R\bar{3}c$ space group. The cell parameters are $a_h = 8.4716(2)$ Å and $c_h = 23.054(1)$ Å.

In Nasicon family, the a_h-parameter depends on the ribbon diameter (i.e. is a function of the A size) and on the interribbon distance (which is related to the amount and to size of the alkali cations in the $M(2)$ or $M(3)$ sites). The comparaison of the a_h-parameters of $Na_3NiZr(PO_4)_3$ ($a_h = 8.8909$ Å), and $Li_{2.6}Na_{0.4}NiZr(PO_4)_3$ ($a_h = 8.4716$ Å), which should have the same ribbon diameter, clearly illusrates the influence of Li^+ insertion in the $M(2)$ or $M(3)$ sites; the decrease of a_h parmeter, when sodium is replaced by lithium in $Na_3NiZr(PO_4)_3$, is related to the size of Li^+ ($rLi^+ = 0.74$ Å) which is smaller than that of Na^+ ion ($rNa^+ = 1.02$ Å) [17]. These results are interpreted based on the fact that, in $Li_{2.6}Na_{0.4}NiZr(PO_4)_3$ phosphate, Na atoms are placed in $M(1)$ site and Li atoms occupy the $M(2)$ or $M(3)$ sites. It should be noticed that this hypothesis was already verified for $Li_{1.6}Na_{0.4}TiM(PO_4)_3$ (M = Fe, Cr) Nasicon phases [19]. The c_h-parameter increases as Li substitutes for Na [$c_h = 22.225$ Å for $Na_3NiZr(PO_4)_3$ and $c_h = 23.054$ Å for $Li_{2.6}Na_{0.4}NiZr(PO_4)_3$]. This behavior results mainly from the Na^+ amount present in the $M(1)$ sites which decreases the O(2)–O(2) repulsions along c-axis. The small difference of c_h-parameters of $Na_3AZr(PO_4)_3$ (A = Mg, Ni) phosphates, can be explained by the slight difference in ionic radii between Mg^{2+} (0.72 Å) and Ni^{2+} (0.70 Å) in octahedral environments.

3.3. Raman investigation

Vibrational spectra have been recorded for all the compositions of the $Na_{1+x}A_{x/2}Zr_{2-x/2}(PO_4)_3$ (A = Mg, Ni) ($0 \leqslant x \leqslant 3$) series and will be published elsewhere [20]. Here we summarized the results obtained for

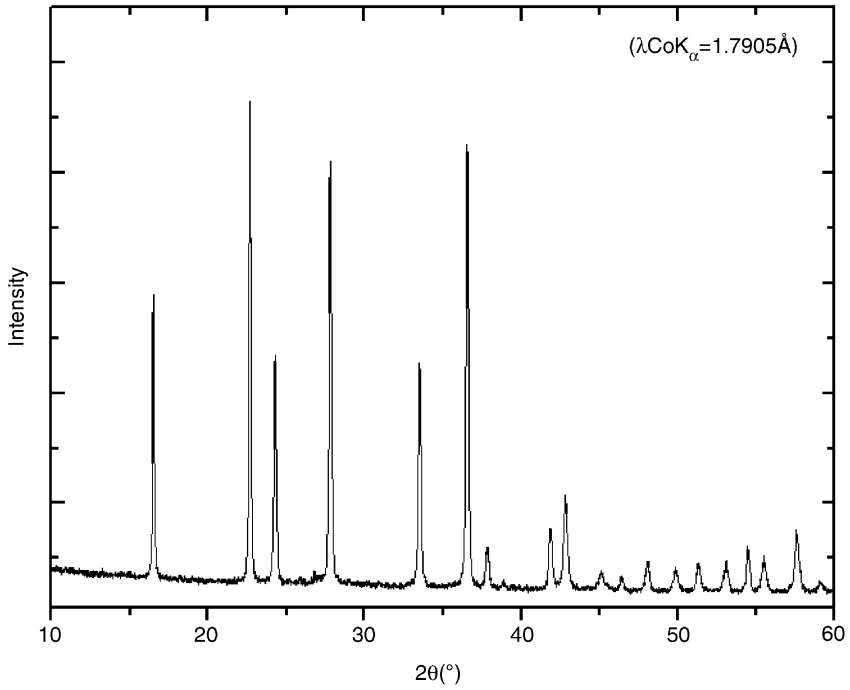

Fig. 4. X-ray diffraction pattern of $Li_{2.6}Na_{0.4}NiZr(PO_4)_3$.

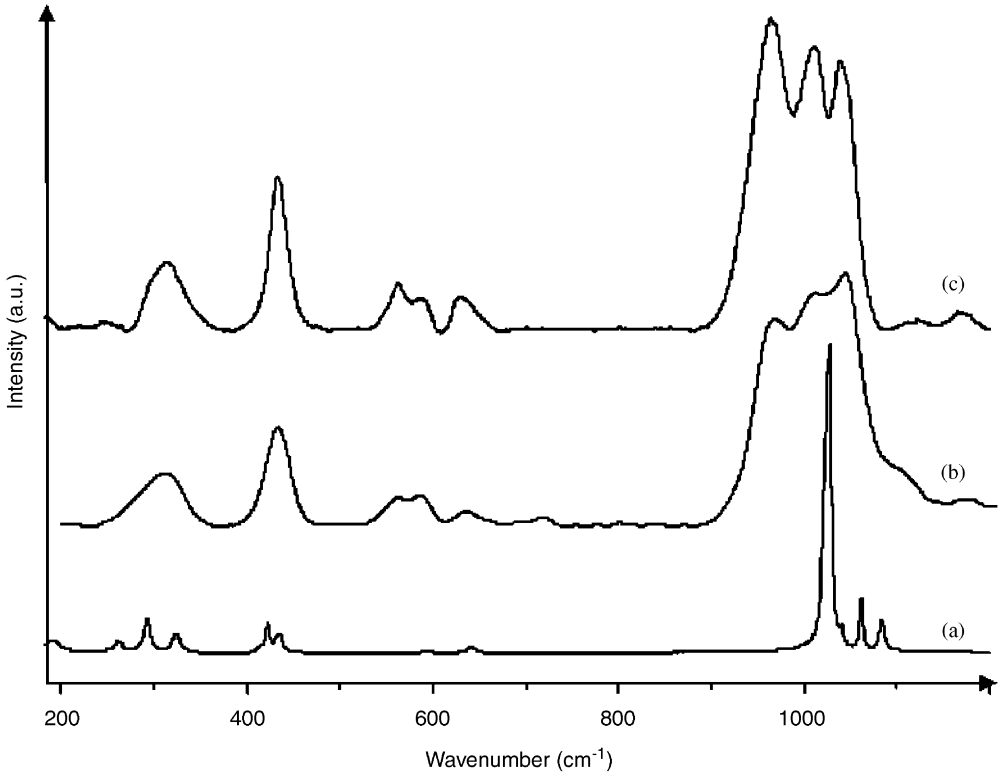

Fig. 5. Raman spectra of $NaZr_2(PO_4)_3$ (a), $Na_3NiZr(PO_4)_3$ (b) and $Na_3MgZr(PO_4)_3$ (c).

$Na_3AZr(PO_4)_3$ (A = Mg, Ni) compositions. Fig. 5 shows their Raman spectra. The high frequency part (900–1200 cm^{-1}) of these spectra corresponds to the stretching vibrations of the PO_4 tetrahedra and exhibits six peaks (Fig. 6) in good agreement with results of the factor group analysis of $R\bar{3}c$. The peaks observed between 700 and 400 cm^{-1} are assigned to the P–O bending vibrations, the predicted ones are eight. The peaks situated below 400 cm^{-1} are attributed to the external modes.

The peaks observed for $Na_3AZr(PO_4)_3$ (A = Mg, Ni) are broader than those obtained for $NaZr_2(PO_4)_3$ [15,21]. In all these phosphates the PO_4 tetrahedra are linked by corners

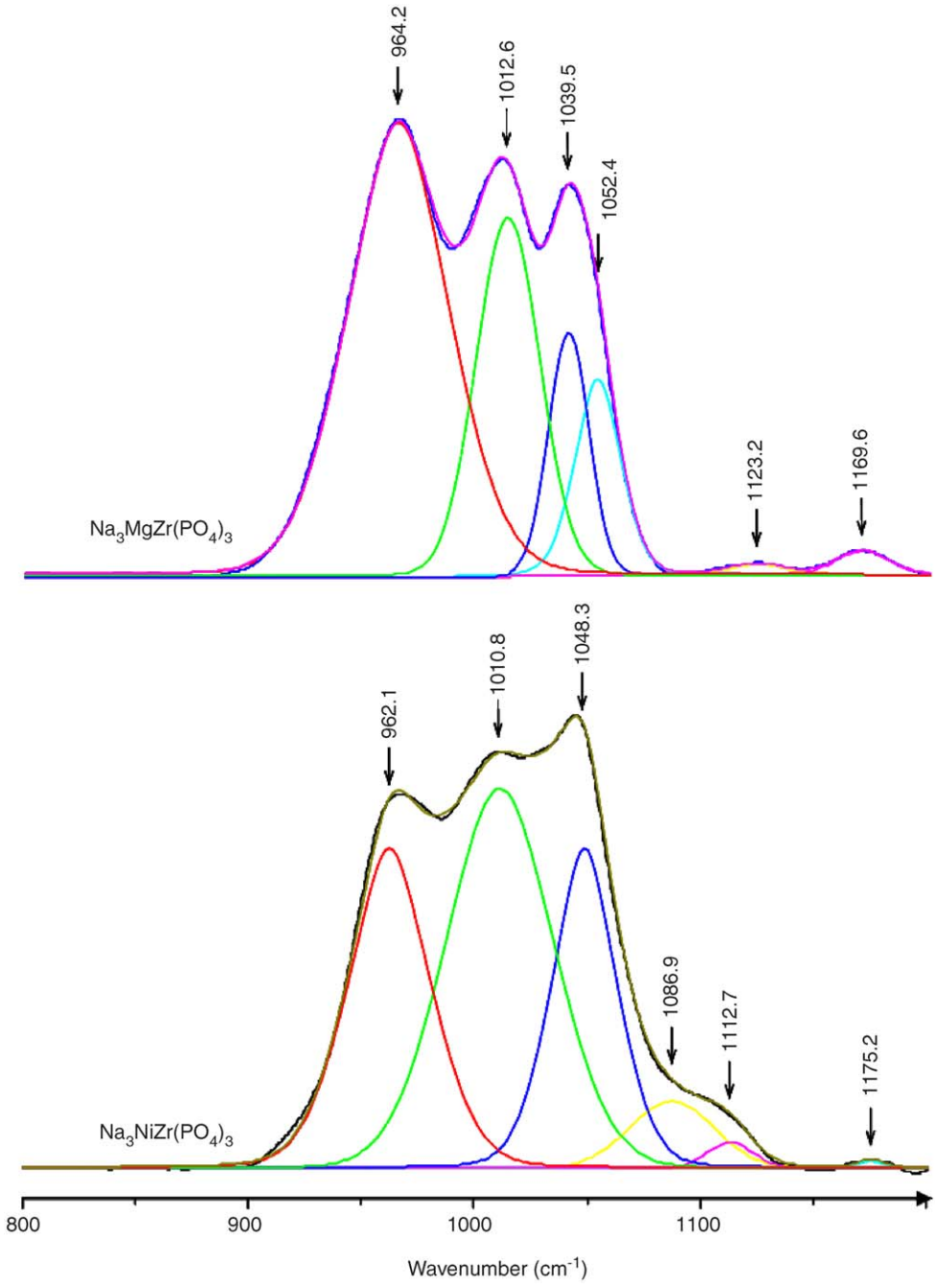

Fig. 6. Raman spectra of $Na_3AZr(PO_4)_3$ (A = Mg, Ni) (range of 800–1200 cm^{-1}).

to Zr/AO_6 (A = Mg, Ni), $Na(1)O_6$ and $Na(2)O_8$ polyhedra. In $NaZr_2(PO_4)_3$ the octahedral site of the framework (12c) is occupied by Zr^{4+} only, $M(1)$ site is totally occupied by Na^+ and $M(2)$ site is totally empty, so there is no disorder around the PO_4 tetrahedra and the Raman peaks are very sharp. In $Na_3AZr(PO_4)_3$ (A = Mg, Ni) the statistical distribution of A^{2+}/Zr^{4+} and Na^+ in 12c and $M(2)$ sites, respectively, induces a disorder around PO_4 tetrahedra and explains the very broad Raman peaks observed for these phosphates.

3.4. Optical properties

Fig. 7 presents the diffuse reflectance spectra of $Na_3AZr(PO_4)_3$ (A = Mg, Ni). The strong band observed at high energy, for both compounds, is due to the electronic transfer from oxygen to zirconium. The optical energy gap values are 4.96 eV for $Na_3NiZr(PO_4)_3$ and 5.06 eV for $Na_3MgZr(PO_4)_3$. These results are in the range usually found for the isostructural phosphate $NaZr_2(PO_4)_3$ (5.06 eV) [22]. The other bands situated in the visible and

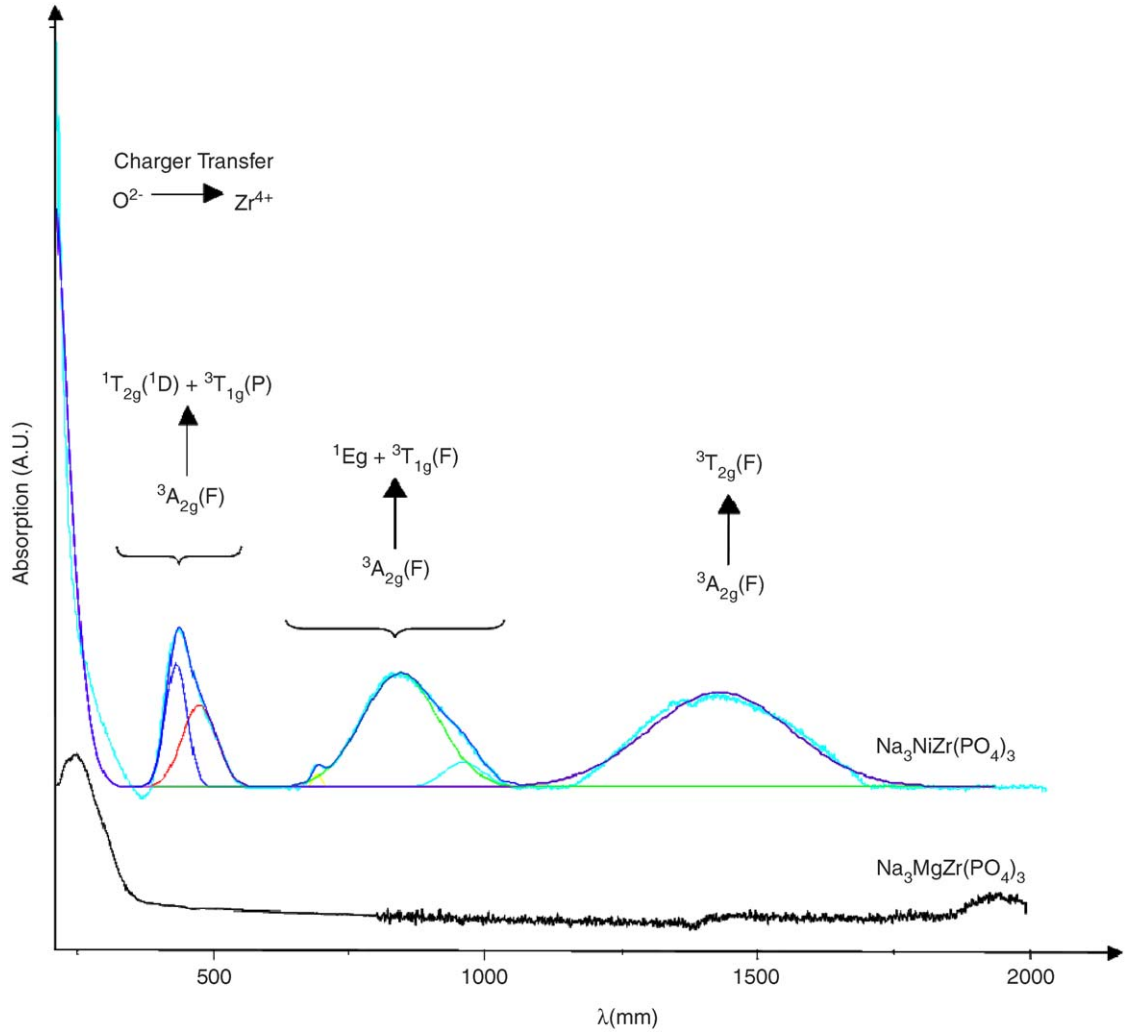

Fig. 7. Diffuse reflectance spectra of $Na_3AZr(PO_4)_3$ (A = Mg, Ni).

Table 5
Experimental and calculated energies of Ni^{2+} transitions in $Na_3NiZr(PO_4)_3$

Transition	Energy (cm^{-1})	
	Obs.	Calc.
$^3A_{2g}(F) \rightarrow {}^3T_{2g}(F)$	6997	7000
$^3A_{2g}(F) \rightarrow {}^3T_{1g}(F)$	11,889	11,668
$^3A_{2g}(F) \rightarrow {}^1E_g$	14,513	14,577
$^3A_{2g}(F) \rightarrow {}^1T_{2g}(^1D)$	21,186	20,618
$^3A_{2g}(F) \rightarrow {}^3T_{1g}(P)$	23,255	24,630

infrared domains, observed only in $Na_3NiZr(PO_4)_3$, are due to d–d transitions of Ni^{2+} in octahedral site. Three broad absorption bands ascribed to the spin-allowed transitions $^3A_{2g} \rightarrow {}^3T_{2g}(F)$, $^3T_{1g}(F)$, and $^3T_{1g}(P)$ were observed at the following frequencies: $\nu_1 = 6997$, $\nu_2 = 11,889$ and $\nu_3 = 23,255\,cm^{-1}$. The spin-forbidden transitions $^3A_{2g} \rightarrow {}^1E_{2g}$, and $^1T_{2g}$ were also observed at $\nu_4 = 14,513$ and $\nu_5 = 21,186\,cm^{-1}$. Table 5 compares the value of the observed and calculated energies. The value of the ligands field parameter (Dq) and Racah parameter (B), calculated by fitting the experimental frequencies to an energy-level diagram for octahedral d^8 systems [23], are $Dq = 700\,cm^{-1}$ and $B = 791\,cm^{-1}$ (for free ion, $B(Ni^{2+})$ is $1041\,cm^{-1}$). These values indicate a weak crystal field for Ni^{2+} and a covalent character of Ni–O bond in good agreement with structural results which showed that Ni^{2+} ions are located in the framework $[NiZr(PO_4)_3]$.

4. Conclusion

A new phosphates $Li_{2.6}Na_{0.4}NiZr(PO_4)_3$ and $Na_3NiZr(PO_4)_3$ have been obtained, respectively, by ion exchange and coprecipitation routes. Structures of $Na_3AZr(PO_4)_3$ (A = Mg, Ni) have been refined from X-ray powder diffraction using Rietveld method. The latter phosphates belong to the Nasicon family and crystallize in the $R\bar{3}c$ space group. A^{2+} (A = Mg, Ni) and Zr^{4+} cations are statistically distributed in the octahedral sites (12c) of the framework. Na atoms occupy partially $M(1)$ and $M(2)$ sites. Raman spectra of these phosphates present broad peaks due to the statistical occupation of the sites

(12*c*, *M*(1) and *M*(2)) around PO_4 tetrahedra. Optical study shows a covalent character of Ni–O bonds.

Acknowledgment

M. Chakir would like to thank the ICMCB Institute, France for their support.

References

[1] Y. Hasegawa, S. Tamura, N. Imanaka, G. Adachi, Y. Takano, T. Tsubaki, K. Sekizawa, J. Alloys Compd. 375 (2004) 212.
[2] A. Aatiq, M. Menetrier, A. El Jazouli, C. Delmas, Solid State Ion. 150 (2002) 391.
[3] T. Alami, R. Brochu, C. Parent, L. Rabardel, G. Le Flem, J. Solid State Chem. 110 (2) (1994) 350.
[4] L.O. Hagman, P. Kierkegaard, Acta Chem. Scan. 22 (1968) 1822.
[5] R. Masse, A. Durif, J.C. Guittel, I. Tordjmman, Bull. Soc. Fr. Mineral. Crystallogr. 95 (1972) 45.
[6] S. Krimi, A. El Jazouli, A. Lachgar, L. Rabardel, D. de Waal, J.R. Ramos-Barrado, Ann. Chim. Sci. Mater. 25 (1) (2000) 75.
[7] S. Krimi, A. El Jazouli, D. de Waal, J.R. Ramos-Barrado, in: Procceding of the Sixth ESG Conference, Montpellier, 2–6 June, 2002.
[8] S. Krimi, I. Mansouri, A. El Jazouli, J.P. Chaminade, P. Gravereau, G. Le Flem, J. Solid State Chem. 105 (1993) 561.
[9] J.P. Boilot, G. Collin, R. Comes, J. Solid State Chem. 50 (1983) 91.
[10] R. Salmon, C. Parent, M. Vlasse, G. Le Flem, Mater. Res. Bull. 14 (1979) 85.
[11] C. Masquelier, C. Wurn, J. Rodriguez-Carvajal, J. Gaubicher, L. Nazar, Chem. Mater. 12 (2000) 525.
[12] J. Gaubicher, C. Wurn, G. Goward, C. Masquelier, L. Nazar, Chem. Mater. 12 (2000) 3240.
[13] S. Barth, M. Andratschke, A. Feltz, C. Jager, Sci. Ceram. 14 (1989) 401.
[14] F. Cherkaoui, Thesis, University of Bordeaux I, 1985.
[15] M. Chakir, Thesis, University of Hassan II-Mohammedia, 2003.
[16] A. Aatiq, Powder Diff. 19 (3) (2004) 272.
[17] R.D. Shannon, Acta Crystallogr. A 32 (1976) 751.
[18] N.E. Brese, M. O'Keeffe, Acta Crystallogr. B 47 (1991) 192.
[19] S. Patoux, G. Rousse, J.B. Leriche, C. Masquelier, Chem. Mater. 15 (2003) 2084.
[20] M. Chakir, A. El Jazouli, D. de Waal, in progress.
[21] P. Tarte, A. Rulmont, C. Merckaert-Ansay, Spectrochim. Acta (A) 42 (9) (1986) 1009.
[22] A. El Jazouli, M. Alami, R. Brochu, J.M. Dance, G. Le Flem, P. Hagenmuller, J. Solid State Chem. 71 (1987) 444.
[23] A.B.P. Lever, Inorganic Electronic Spectroscopy, Elsevier, Amsterdam, 1984.